In L.A. Clark, ed., Gold in the Western Shield, Canadian Institute of Mining and Metallurgy, Sp. Vol. 38, 1986.

THE GEOLOGIC SOLUBILITY OF GOLD FROM 200-350°C, AND ITS IMPLICATIONS FOR GOLD-BASE METAL RATIOS IN VEIN AND STRATIFORM DEPOSITS

L.M. Cathles
Chevron Oil Field Research Company
P.O. Box 446
La Habra, CA 90631

ABSTRACT

Silicate and sulfide buffers that control the major element chemistry and pH of geothermal solutions in common geologic environments are used to investigate the "geologic" solubility of gold as a function of temperature and solution salinity. The geologic solubility of gold is much greater in low-salinity solutions, and for any given salinity is probably maximum at about 300°C. The selectivity of low-salinity solutions for gold and against base metals (which are carried as chloride complexes), and conversely, the selectivity of higher salinity solutions for base metals and against gold, explains the distinct bimodal metal contents of vein and stratiform deposits which have either high gold and little or no base metals, or lower gold and abundant base metals. The 300°C maximum in gold solubility could explain why gold veins tend to have somewhat lower maximum temperatures of formation than base metal veins and massive sulfie deposits. A basin evolution model is suggested that can account for both the metal ratios and locations of gold and base metal deposits in greenstone belts.

INTRODUCTION

It has been proposed that gold deposits are produced by the venting of magmatic fluids (eg. porphyry gold systems, Henley and Ellis, 1983), by convecting hydrothermal systems in subaerial settings (eg, the Taupo Rift Zone and its fossil analogues in New Zealand, Henley and Ellis, 1983), and by metamorphic dewatering (eg., greenstone-hosted gold deposits, Fyfe and Kerrich, 1983). The magmatic case is distinctive because magamatic fluids originate at higher temperatures, and because gold is probably precipitated where the magmatic fluids condense rather than decompress or boil. This paper focusses on gold deposited from non-magmatic (formation) waters.

It is convenient to distinguish the two kinds of non-magmatic gold veins. Gold veins in greenstone belts that hypothetically precipitate from venting metamorphic fluids will be referred to as "greenstone-hosted" deposits. Gold veins which precipitate from boiling fluids convecting in subaerial settings will be referred to as "epithermal gold" deposit.

Both epithermal and greenstone-hosted gold veins are remarkably low in base metals. Fyfe and Kerrich (1983) have pointed out that some greenstone-hosted gold

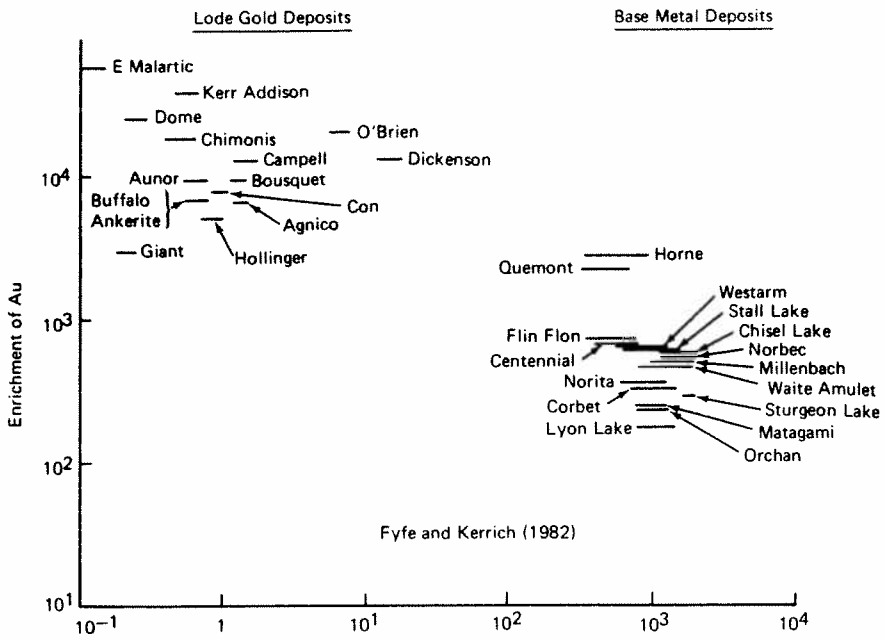

Fig. 1 *The enrichment of gold and Cu + Zn in greenstone-hosted gold and base metal deposits relative to unaltered igneous rocks. The distinct bimodal populations require selection for gold and rejection of base metals in the lode gold deposits, and selection for base metals and relative rejection of gold in the massive sulfide deposits. Figure is from Fyfe and Kerrich (1983, Figure 4).*

deposits contain less base metal than unaltered igneous rocks; at the same time they are strongly enriched in gold (see Figure 1). The lack of base metal is not due to absence of a leachable source. The Archean greenstone belts that contain the gold deposits also contain copper and zinc massive sulfide deposits (Figure 2), although the gold and base metal deposits tend to be separated geographically. The same is true of epithermal vein deposits. Epithermal base metal veins are generally not rich in gold, although gold may be a by-product. Epithermal gold veins tend to be low in base metals, although they may contain a few percent pyrite.

The distinct geochemical separation of deposits into two categories, gold-rich and base metal-poor, and base metal-rich and relatively gold-poor, requires that the hydrothermal fluids responsible for the gold deposits select (either in their transport or deposition) strongly for gold and against base metals, and that the solutions responsible for the base metal deposits do the converse—select strongly for base metals and against gold. This paper shows that the selectivity can be achieved by differences in the solubility of base and precious metals in the source solutions.

Drummond and Ohmoto (1985) have modeled precipitation of precious and base metals during boiling. They argue that almost all base and precious metals are precipitated from hydrothermal solutions by the time 10 wt% of the liquid is lost to steam. Recent work in New Zealand indicates that the hydrothermal solutions

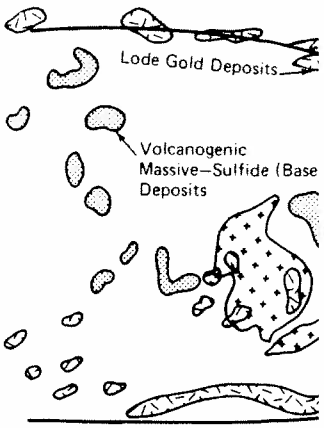

Fig. 2 *The distribution of lo greenstone belt, Quebec. Gene Drolet (1981).*

there are nearly saturated wit when the solutions lose H_2S dicates that the availability o Zealand, and confims that precipitates gold. If boiling p from a hydrothermal solution, mal vein deposits. If scarce me systems as the New Zealand d in the more abundant base m is thus not the likely cause of argued that the chemistry of or precious metals is, by defa cumulation of metals in epithe is geochemically reasonable.

THE EQUILIBRIUM CONC SOLUTIONS

The Problem with Relating

In moderate temperature (~ ried as bisulfide complexes (S

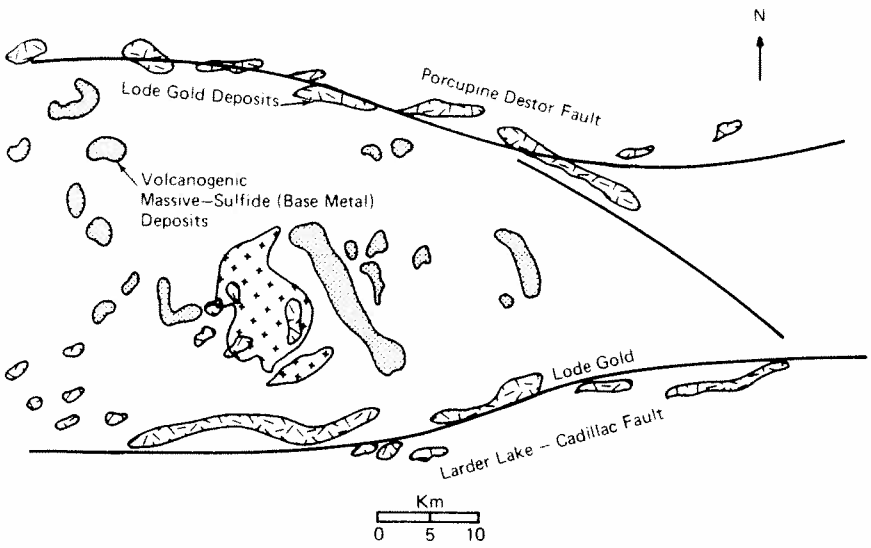

Fig. 2 *The distribution of lode gold and massive sulfide deposits in the Abitibi greenstone belt, Quebec. Generalized from map compiled by Avramtchev and Lebel-Drolet (1981).*

there are nearly saturated with gold and that essentially all the gold precipitates when the solutions lose H_2S during decompression (Brown, submitted). This indicates that the availability of leachable gold is not a problem, at least in New Zealand, and confims that boiling (to atmospheric pressure) quantitatively precipitates gold. If boiling precipitates nearly all the base and precious metals from a hydrothermal solution, it cannot be the cause of metal selectivity in epithermal vein deposits. If scarce metals like gold are typically saturated in hydrothermal systems as the New Zealand data suggests, the solutions are likely to be saturated in the more abundant base metals also. The availability of gold and base metals is thus not the likely cause of metal selectivity either. Consequently it could be argued that the chemistry of the hydrothermal solutions where they leach base or precious metals is, by default, the best candidate for the observed selective accumulation of metals in epithermal and lode gold deposits. This paper shows this is geochemically reasonable.

THE EQUILIBRIUM CONCENTRATION OF GOLD IN HYDROTHERMAL SOLUTIONS

The Problem with Relating Gold Solubility to Eh, pH, m_{H_2S} and T:

In moderate temperature (~ 300°C) reduced hydrothermal solutions gold is carried as bisulfide complexes (Seward, 1973; Henley et al, 1984). Under conditions

where the $Au(HS)_2^-$ complex dominates, gold solubility may be calculated from experimentally-determined (Seward, 1973, Table 4) equilibrium constants for the following reaction:

[1] $Au^\circ + H_2S + HS^- = Au(HS)_2^- + 0.5\ H_2(g)$

If the partial pressure of hydrogen is related to oxygen fugacity through the reaction for the breakdown of water, and HS^- is related to H_2S and pH by the reaction for the dissociation of H_2S ($H_2S = HS^- + H^+$), using an approximate log activity coefficient for $Au(HS)_2^-$ of -0.168 and a unit activity of water, the solubility of gold as the $Au(HS)_2^-$ complex may be written:

$$[2]\quad \log m_{Au(HS)_2^-} = \begin{matrix} 3.35 \\ 1.46 \\ -0.08 \\ -1.36 \end{matrix} + pH + 0.25 \log f_{O_2} + 2 \log m_{H_2S}$$

The vector of constants in the above equation refers, from the top down, to 200, 250, 300 and 350°C; m is molality, and f_{O_2} is the fugacity of oxygen. Values of the water and H_2S dissociation reactions used in calculating the constants were taken from Henley et al (1984). This reference supplies details and refiements of this method of computing gold solubility. If temperature, pH, f_{O_2}, and m_{H_2S} are known, equation (2) allows the gold solubility to be easily calculated. Figure 3 shows the result for pH=7, log f_{O_2}=-35, and m_{H_2S}= 100 ppm. Figure 3 shows that gold solubility strongly decreases, under these conditions, as temperature increases.

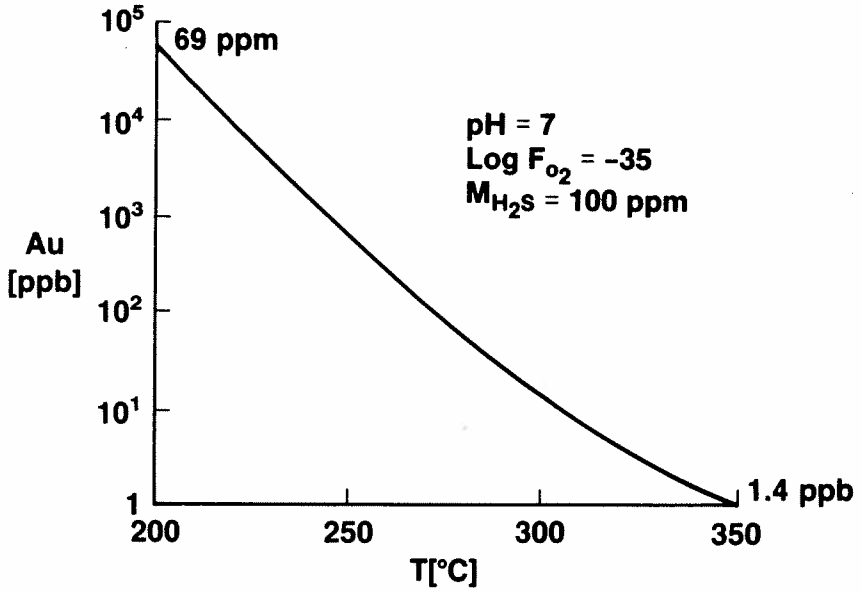

Fig. 3 *Gold solubility calculated from equation [2] for specific values of* f_{O_2}, m_{H_2S}, *and pH with temperature.*

The problem is, of course
tant complex under the spec
f_{O_2} and m_{H_2S} may all chan
geological environments to p
such as Figure 3 (in fact tl

Gold Solubility in Silicat

A better approach to estir
of chemical equilibria to
temperature and the indepe
the first to utilize this appro
Giggenbach (1981) has gene
in hydrothermal solutions. A
equilibria control all major
and have identified the equi
norsson et al 1983a, b). Re
composition of hydrotherm

The equilibria that Ellis,
portant in controlling hydr
in geochemical computer p
the minerals we have chose
thermal solutions. The therm
ed in the appendix. Tempe
cations are controlled by th
quartz and calcite. The redo
(ca-chlorite), and magnetit
following discussion this
hydrothermal chemistry to d
EQ3's simulation of gold so
model of Table 1 is used to
solutions as a function of te
results are discussed.

Verification of the Equilib of Natural Hydrothermal

Table 2 compares the
Broadlands, New Zealand,
for the temperatures and sa
the non-volatile species an

Figure 4 compares Na, K
(augmented by data from tl
the EQ3 calculations for th

The problem is, of course that even assuming that $Au(HS)_2^-$ is the only important complex under the specified conditions (which is roughly true), the pH, log f_{O_2} and m_{H_2S} may all change strongly enough as a function of temperature in geological environments to preclude drawing any *geologic* conclusions from figures such as Figure 3 (in fact they do).

Gold Solubility in Silicate- and Sulfide-Buffered Solutions:

A better approach to estimating the geologic solubility of gold takes advantage of chemical equilibria to define how pH, H_2S and f_{O_2} vary as a function of temperature and the independent chemistry of the fluid. Ellis (1970) was perhaps the first to utilize this approach. It is the basis for the Na-K-Ca geothermometer. Giggenbach (1981) has generalized it to include the concentration of H_2S and CO_2 in hydrothermal solutions. Arnorsson and coworkers have demonstrated that mineral equilibria control all major components in geothermal solutions except chloride, and have identified the equilibria that are most important (Arnorsson, 1983; Arnorsson et al 1983a, b). Reed and Spycher (1984) illustrate the mineral-buffered composition of hydrothermal solutions in a particularly instructive way.

The equilibria that Ellis, Giggenbach, Arnorsson and Reed have shown are important in controlling hydrothermal solution chemistry can be easily expressed in geochemical computer programs such as EQ3 (Wolery, 1983). Table 1 shows the minerals we have chosen to constrain the chemistry of the calculated hydrothermal solutions. The thermodynamic data base used in the calculations is discussed in the appendix. Temperature and salinity ($m_{\Sigma Cl}$) are specified. The major cations are controlled by the aluminosilicates. Silica and $CO_3^{=}$ are controlled by quartz and calcite. The redox state, iron, and H_2S are controlled by pyrite, daphnite (ca-chlorite), and magnetite. Electrical charge balance determines pH. In the following discussion this model is first verified by comparing its predicted hydrothermal chemistry to data from geothermal systems and Giggenbach's model. EQ3's simulation of gold solubility experiments is then verified. Finally the EQ3 model of Table 1 is used to study the geologic solubility of gold in hydrothermal solutions as a function of temperature and salinity, and the implications of these results are discussed.

Verification of the Equilibrium EQ3 Model Against the Observed Chemistry of Natural Hydrothermal Systems

Table 2 compares the observed deep (pre-boiled) solution chemistry at Broadlands, New Zealand, and at Mahio, Philippines to the chemistry calculated for the temperatures and salinities of these systems. Agreement is excellent for the non-volatile species and H_2S; fair for CO_2.

Figure 4 compares Na, K, Ca, and pH data from geothermal wells in Iceland (augmented by data from the New Zealand and Philippine wells in Table 2) to the EQ3 calculations for the model in Table 1. Agreement is good.

Table 1

Contraints that allow the equilibrium chemistry and gold solubility of hydrothermal solutions to be calculated by EQ3 (Wolery, 1983) as a function of temperature and m_{Cl^-}.

T	specified
m_{Cl^-}	specified
m_{Na^+}	equilibrium with albite
m_{K^+}	" " muscovite
$m_{Ca^{++}}$	" " wairakite
$m_{Al^{+++}}$	" " k-feldspar
$m_{SiO2(aq)}$	" " quartz
$m_{CO3^{--}}$	" " calcite
$m_{Fe^{++}}$	" " 14A-daphnite
$m_{Fe^{+++}}$	" " magnetite
m_{HS^-}	" " pyrite
m_{Au^+}	" " gold
m_{Ag^+}	" " acanthite
pH	charge balance

Figure 5 shows the Table 1 EQ3 model predicts the chemistry and pH of geothermal systems well at low salinities, but tends to predict too high concentrations of Na plus K for the predicted pH at higher salinities and temperatures. Loss of accuracy in the Debye Huckel activity coefficients at high salinities may be the cause of this discrepancy. Choosing different (but still reasonable) buffer minerals such as high albite, high sanidine, or zoisite does not help. The discrepancies at higher salinities do not affect the conclusions of this paper.

Figure 6 shows that for T $\leq$300°C the calculated (Table 1 EQ3 model) H_2S concentrations in pre-boiled hydrothermal solutions agree well with Giggenbach's (1981) model and with Arnorsson et al's (1983a) geothermal data. At temperatures above 300°C the EQ3 model diverges from Giggenbach's model and perhaps from the geothermal data. The agreement between the EQ3 model and geothermal observations indicates the pyrite-daphnite-magnetite buffer is not inappropriate. The H_2S concentrations would not be significantly different (ie. would plot at nearly the same locations in Figure 6) if pyrrhotite were used as a buffer mineral instead of 14A-daphnite. The H_2S concentrations are decreased but show the same form if hematite is substituted for magnetite as a buffer mineral.

Comparison of calculated and
in two geothermal fields. Data f
et al (1984, Figure 7.1). Activity
assuming Na^+, K^+ and Ca^{++}
portions as in the calculations
for the locations are plotted i

Broadlands, New Zealand

	T[°C]	ΣCl[ppm]	pH	ΣNa[ppm]
obsv	261°C	1238	6.3	705
calc	261°C	1238	6.7	751

Mahio, Philippines

obsv	324°C	9124	5.8	5018
calc	324 °C	9124	5.8	4908

The choice of daphnite as a b
(1980), dictated by increase in
temperature in geothermal syste
calculated for the model in Tab
systems. The trend of the calcula
if pyrrhotite is used instead of d
common alteration mineral in h

Figure 8 compares the H_2CO_3
plagioclase-calcite-clay model ar
in geothermal systems. H_2CO_3 cc
tant as a general check on the v
interest in this paper). They are
boiling begins, but are significant
250°. Our model agrees well witl
bach's have a different temperatu
the data and models agree fairly
model depend on the extrapolati
220°C to higher temperatures (se
between the theoretical H_2CO_3 ca
investigation, but is not critical t
does not depend on CO_2 chemis

Figures 4-8 show the model o
boiled solutions in presently-acti
ches the geochemistry and pH o
Cl) salinities and has the correct g
ty. Individual geothermal systems
Figure 11 and Ragnarsdottir et al
that most silicate minerals have sin

Table 2

Comparison of calculated and observed deep (pre-boiled) geothermal fluids in two geothermal fields. Data from Henley and Hedenquist (1983) and Henley et al (1984, Figure 7.1). Activity ratios for the observed data were calculated assuming Na^+, K^+ and Ca^{++} exist in the natural solutions in the same proportions as in the calculations; the observed and calculated activity ratios for the locations are plotted in Figure 4.

Broadlands, New Zealand

	T[°C]	ΣCl[ppm]	pH	ΣNa[ppm]	ΣK[ppm]	ΣCa[ppm]	H_2S[ppm]	CO_2[ppm]
obsv	261°C	1238	6.3	705	150	5.0	72	4,104
calc	261°C	1238	6.7	751	104	6.5	50	139

Mahio, Philippines

obsv	324°C	9124	5.8	5018	1379	122	85	2,945
calc	324 °C	9124	5.8	4908	1428	269	104	11,682

The choice of daphnite as a buffer mineral is, as pointed out by Giggenbach (1980), dictated by increase in the m_{H_2}/m_{H_2S} ratio observed with increasing temperature in geothermal systems. Figure 7 shows the variation in this ratio, calculated for the model in Table 1, is similar to that observed in geothermal systems. The trend of the calculated curves does not agree with the observed data if pyrrhotite is used instead of daphnite. Perhaps most importantly chlorite is a common alteration mineral in hydrothermal systems, pyrrhotite is not.

Figure 8 compares the H_2CO_3 concentration predicted by Giggenbach's (1981) plagioclase-calcite-clay model and the EQ3 model of Table 1 to values observed in geothermal systems. H_2CO_3 concentrations in geothermal solutions are important as a general check on the validity of solution chemistry models (our main interest in this paper). They are also important in controlling the depth at which boiling begins, but are significant in this regard only at temperatures greater than 250°. Our model agrees well with Giggenbach's but both our model and Giggenbach's have a different temperature trend than the geothermal data. Nevertheless the data and models agree fairly well at temperatures above 250°. Results in our model depend on the extrapolation of the dissociation constant for H_2CO_3 from 220°C to higher temperatures (see appendix discussion). The difference in trend between the theoretical H_2CO_3 calculations and geothermal data warrants further investigation, but is not critical to our present purposes because gold solubility does not depend on CO_2 chemistry.

Figures 4-8 show the model of Table 1 simulates the chemistry of deep pre-boiled solutions in presently-active geothermal systems reasonably well. It matches the geochemistry and pH of geothermal systems well at low (~ 1000 ppm Cl) salinities and has the correct general dependence of pH and chemistry on salinity. Individual geothermal systems may vary slightly from this general model (see Figure 11 and Ragnarsdottir et al., 1984). Arnorsson has pointed out, however, that most silicate minerals have similar solubilities. This means minerologic or rock

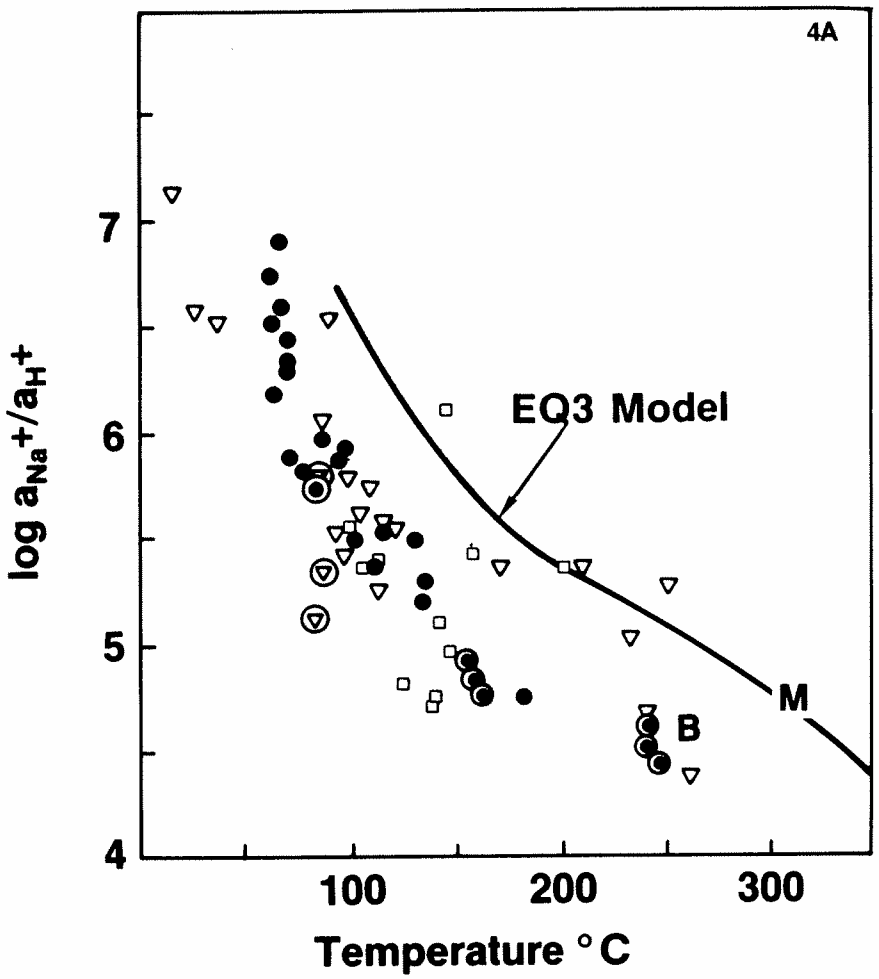

Fig. 4A,B,C *Activities of aqueous species in geothermal waters from Iceland, measured by Arnorsson et al (1983), are compared to the activities predicted by the EQ3 model of Table 1. Filled circles represent unmixed drillhole discharges and are the most reliable data. Triangles represent mixed drillhole discharges and non-boiling hot springs, squares boiling hot springs. The two analyses from New Zealand (Broadlands) and the Phillippines (Mahio) listed in Table 2 have been added to Arnorsson et al's original diagrams, assuming the activity of coefficients are as calculated by the EQ3 model for the temperatures and salinities of these locations. The curves predicted by the EQ3 model of Table 1 have also been added to the diagram. The salinity of the Iceland waters plotted in this figure are generally low (less than a few hundred ppm Cl, Arnorsson et al, 1983a, Table 2 and 3).*

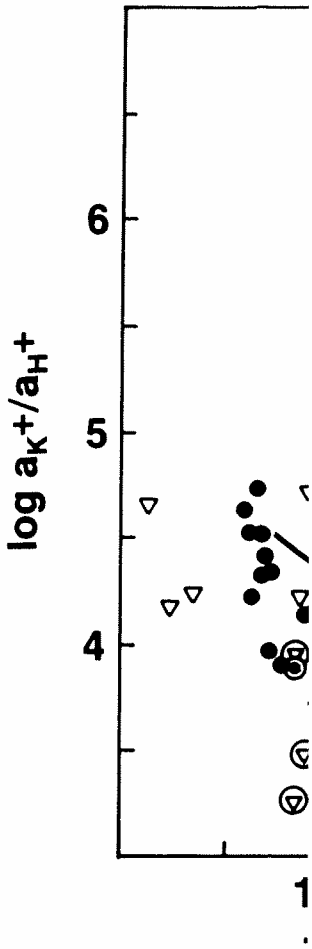

type differences have only a
1983; Arnorsson et al, 1983
on alteration at temperatu
permeability. The alteratio
Iceland, the rhyolites of Ne
temperatures, rock type d
minerology (ie., low silica
The H_2S concentration dict
pears to be relatively insensi
The model in Table 1 is thu
systems and consequently p
vestigate the geologic solut

Figure 9 demonstrates tha
bisulfide complexes are inc

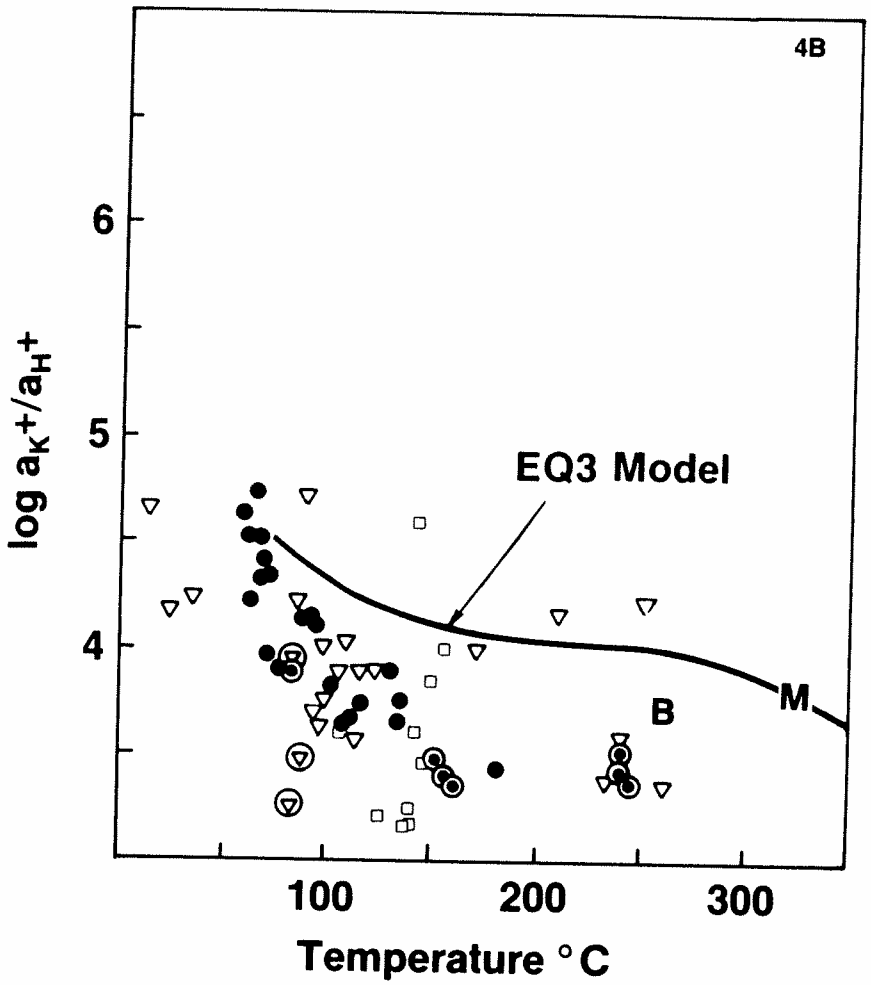

type differences have only a minor influence on solution chemistry (Arnorsson, 1983; Arnorsson et al, 1983a). Brown (1978) states the main influence of rock type on alteration at temperatures above about 280°C is through differences in permeability. The alteration mineral assemblage is the same in the basalts of Iceland, the rhyolites of New Zealand, and the andesites of Indonesia. At lower temperatures, rock type dictates only fairly minor differences in alteration minerology (ie., low silica zeolites in basalts, high silica zeolites in ryholites). The H_2S concentration dictated by the pyrite-daphnite-magnetite buffer also appears to be relatively insensitive to geologically reasonable changes in that buffer. The model in Table 1 is thus robust and supported by observations in geothermal systems and consequently provides a reasonable background against which to investigate the geologic solubility of gold.

Figure 9 demonstrates that when Seward's (1973) dissociation constants for gold bisulfide complexes are incorporated into the EQ3 data base, the EQ3 program

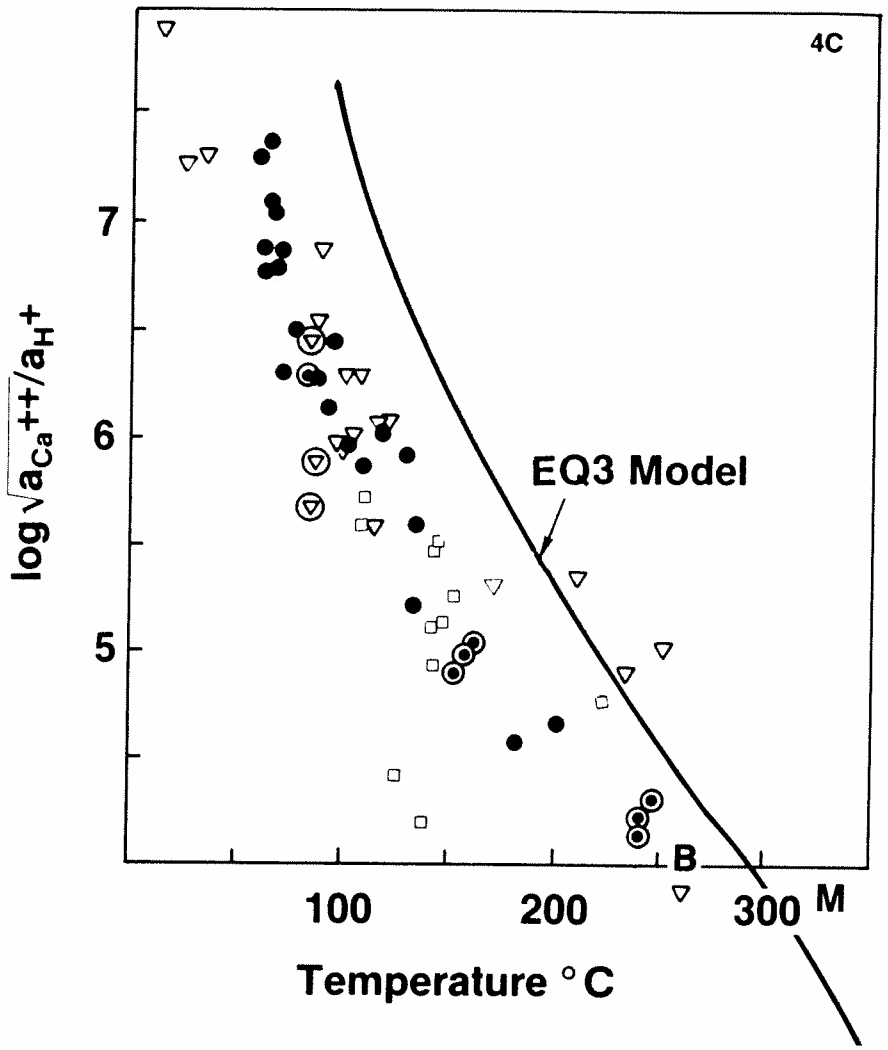

adequately simulates Seward's experimental results. The dissolution constants for the $HAu(HS)_2^\circ$ complex have been deduced from Seward's paper (Figure 6), and are given, with others, in the appendix.

The Geologic Solubility of Gold as a Function of Temperature and Salinity:

Figure 10 shows the silicate- and sulfide-buffered (Table 1 EQ3 model) solubility of gold as a function of temperature for 1000 ppm Cl^- solutions. The solubility of gold increases with increasing temperature up to about 300°C and then decreases sharply as temperature increases further. The increase to 300°C is due primarily to the increased solubility of Au^+ and HS^-. The drop above 300°C results from a sharp decrease in the concentration of the HS^- gold ligand. The drop in HS^-

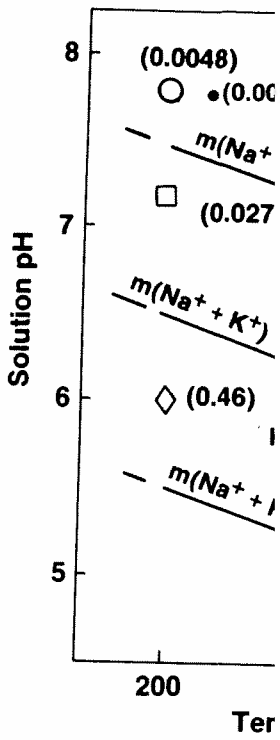

Fig. 5 *The pH and m_{Na^+} plu predictions of the emperic predictions of the EQ3 mo deteriorates at higher salini et al (1984).*

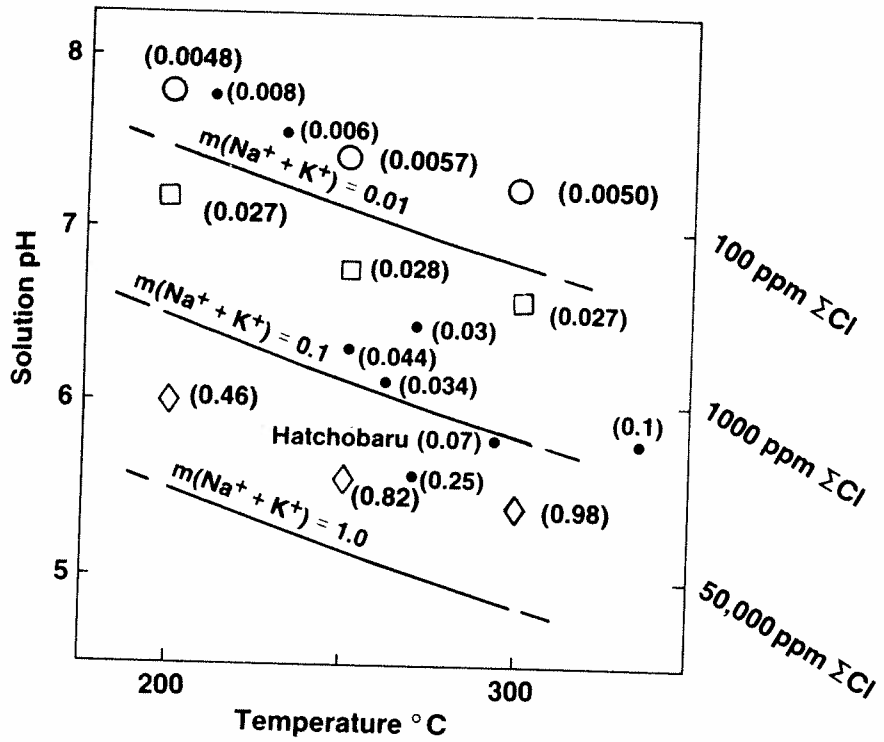

Fig. 5 *The pH and m_{Na} plus m_K values of geothermal wells (solid points) and the predictions of the emperical Na-K geothermometer (lines) are compared to the predictions of the EQ3 model of Table 1. Agreement is good at low salinities but deteriorates at higher salinities and temperatures. The base diagram is from Henley et al (1984).*

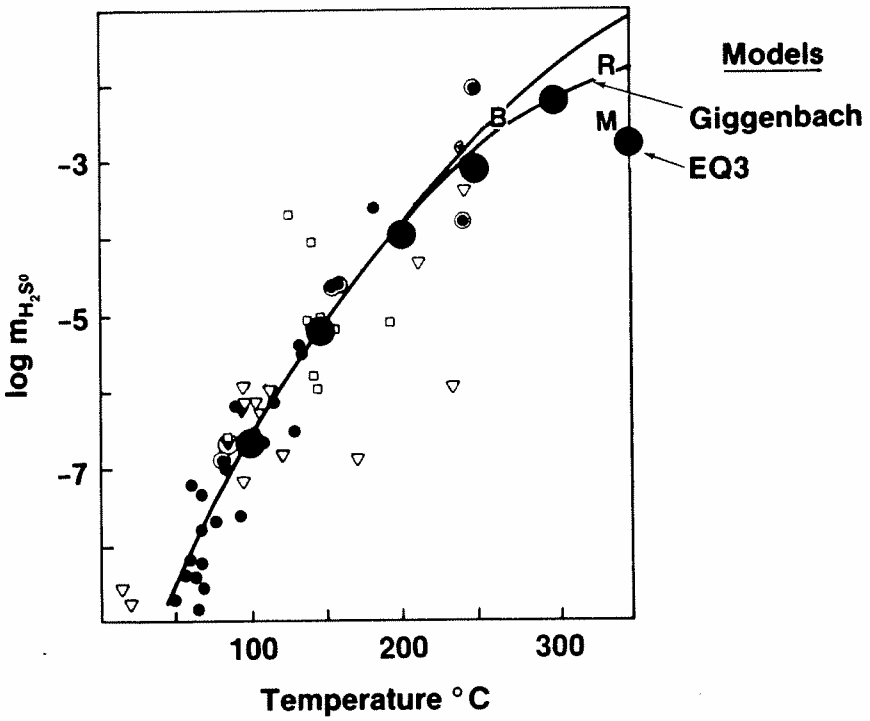

Fig. 6 *m_{H_2S} in Iceland geothermal solutions (from Arnorsson et al, 1983) compared to the equilibrium concentrations predicted by Giggenbach (1981; P_{H_2S} converted to H_2S[aq] using Henries Law constants from Drummond, 1981) and the EQ3 model in Table 1. The upper solid line is a best fit to the observed geothermal data (Arnorsson et al, 1983a, Table 5). Data symbol conventions are the same as in Figure 4. R is data from deep unboiled fluids at Rotakawa, New Zealand (324°C, 600-700 ppm H_2S, Seward, p.c., August 1985).*

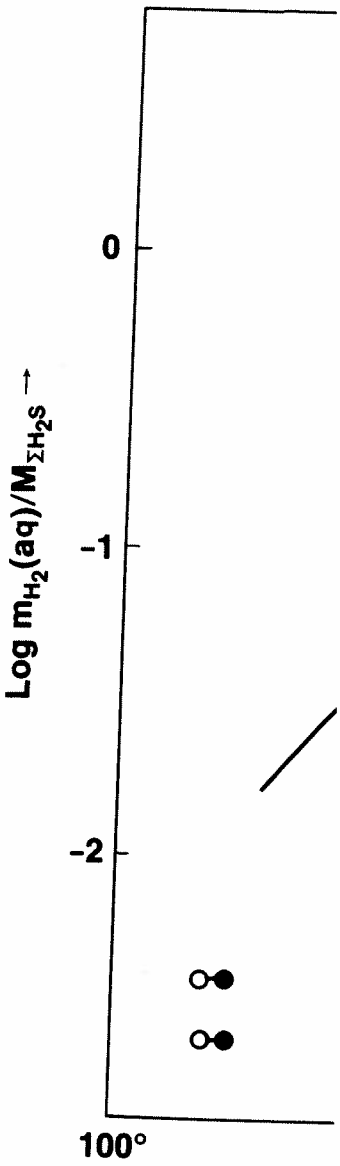

Fig. 7 *Comparison of the H_2/H_2S genbach, 1980) to that calculated about 200°C the molal concentr geothermal data measures H_2S reasonable), the Table 1 model thermal data.*

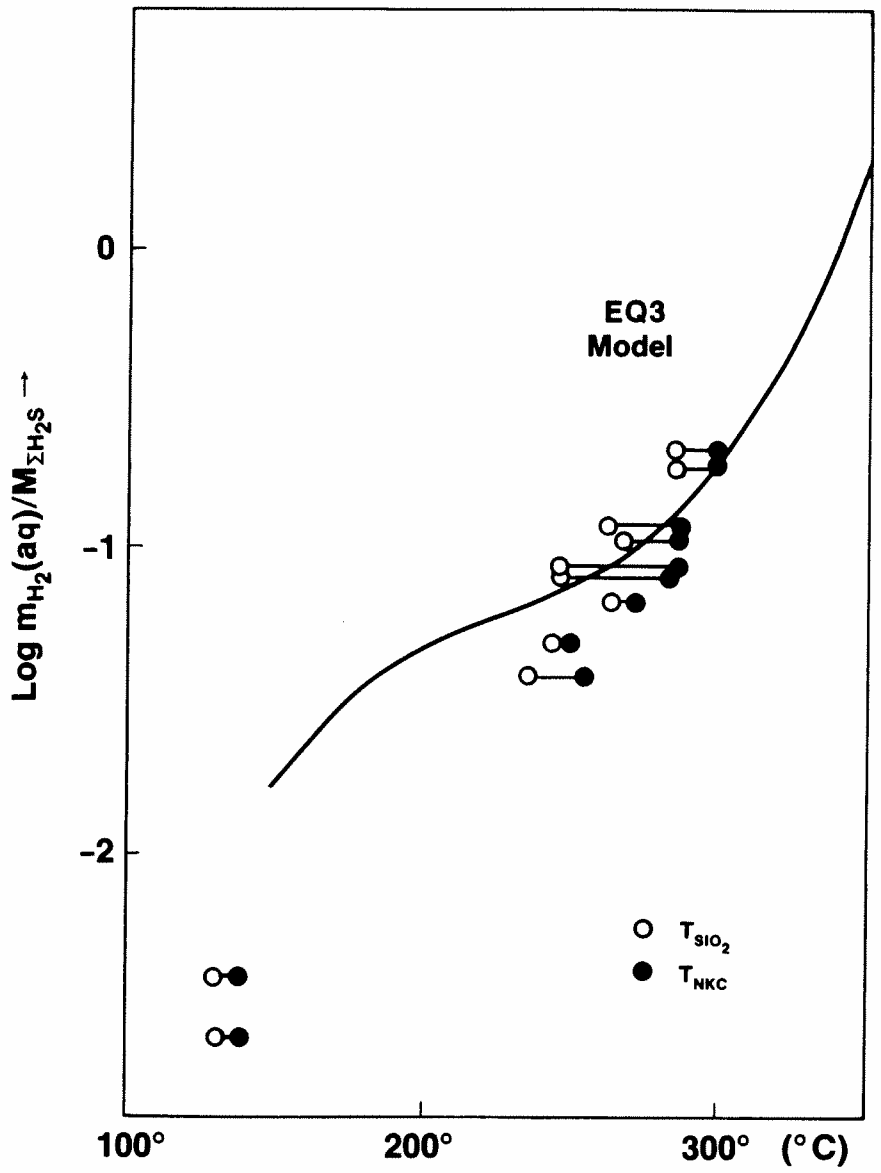

Fig. 7 *Comparison of the H_2/H_2S+HS^- ratio observed in geothermal systems (Giggenbach, 1980) to that calculated by the Table 1 EQ3 model. At temperatures below about 200°C the molal concentrations of HS^- exceeds that of H_2S. Assuming the geothermal data measures H_2S+HS^- (which given the measurement method is reasonable), the Table 1 model provides a good simulation of the observed geothermal data.*

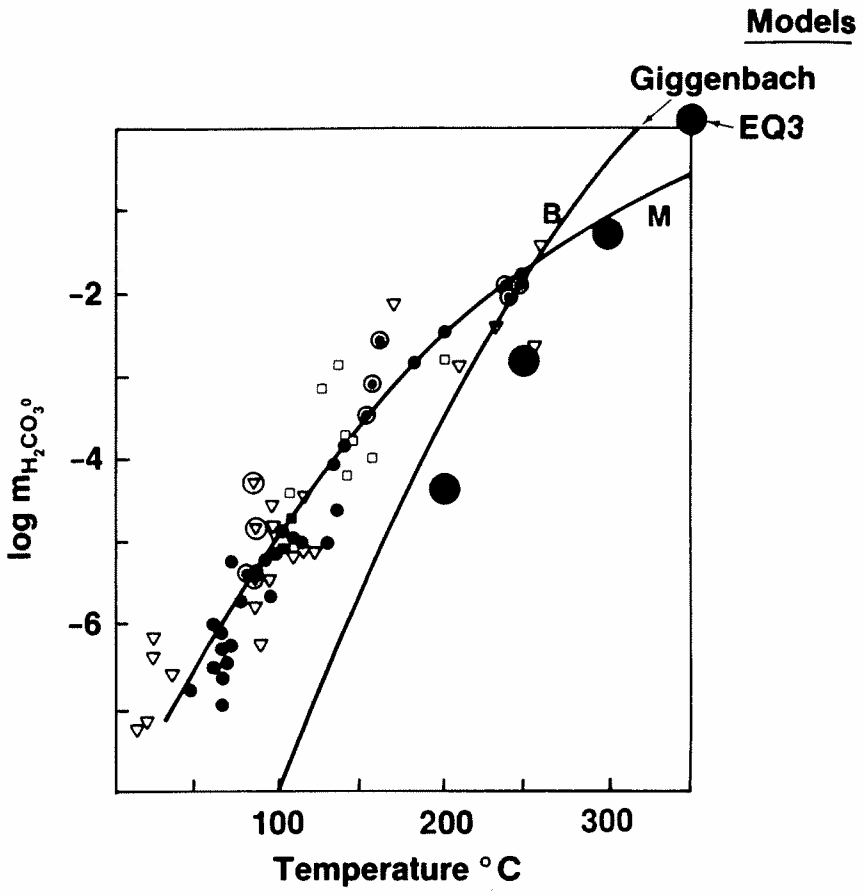

Fig. 8 *$m_{H_2CO_3}$ in Iceland geothermal solutions (from Arnorsson et al, 1983) compared to the equilibrium concentrations predicted by Giggenbach (1981); P_{CO_2} converted to $m_{\Sigma CO_2}[aq]$ using α in Elder, 1981, p204) and the EQ3 model in Table 1. Data symbol conventions are the same as in Figure 4. The unlabelled solid line is a best fit to the geothermal data (Arnorsson et al, 1983a, Table 5).*

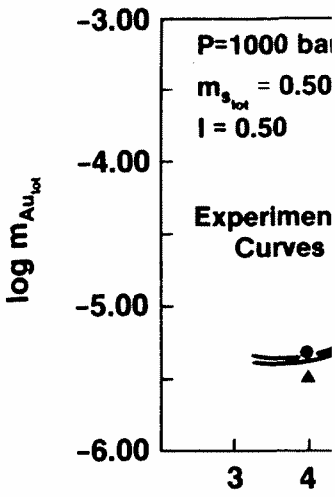

Fig. 9 *Experimental gold co to the gold concentrations pr tions (T, pH, and $m_{\Sigma S}$ speci appendix for the gold bisulfi*

concentration between 300 a dissociation constant (appen in pH (Figure 5), and half f 300°C (Figure 6).

A drop or at least plateauin appears fairly certain. The temperature rests on a clear 276°C (see appendix discuss trend (Figure 6), this increas by the decrease in the H_2S di centrations would still drop. If 6), the geologic solubility of dissociation constant to better solubility of gold unchanged

The cause of the geologic are apparent from the calcul the solubility of gold as indi than suggested by Figure 3 n (which by equation (2) decrea and because the activity of H_2 the solubility of gold by 3 o

Figure 11 shows the solubil solubility is greatly enhance greater concentrations of the

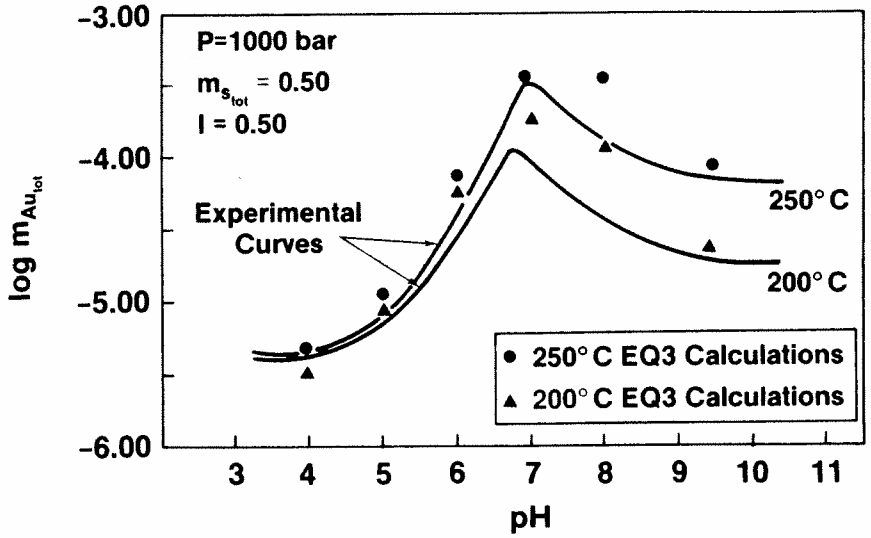

Fig. 9 *Experimental gold concentrations measured by Seward (1973) compared to the gold concentrations predicted by EQ3 under the same experimental conditions (T, pH, and $m_{\Sigma S}$ specified; equilibrium with pyrite and pyrrhotite). See appendix for the gold bisulfide dissociation constants used in the calculations.*

concentration between 300 and 350°C results half from a decrease in the H_2S dissociation constant (appendix), offset slightly by a small (0.08 unit) decrease in pH (Figure 5), and half from a decrease in the concentration of H_2S above 300°C (Figure 6).

A drop or at least plateauing of geologic gold bisulfide solubility above ~300°C appears fairly certain. The decrease in the H_2S dissociation constant with temperature rests on a clear extrapolation of experimental data covering 20° to 276°C (see appendix discussion). If H_2S increases acording to the Giggenbach trend (Figure 6), this increase above 300°C would still be more than outweighed by the decrease in the H_2S dissociation constant above 300°C; HS^- and Au concentrations would still drop. If the H_2S trend is that indicated by Arnorsson (Figure 6), the geologic solubility of gold would plateau at ~300°C. Changing the H_2S dissociation constant to better fit Arnorsson's H_2S trend would leave the retrograde solubility of gold unchanged (see appendix discussion).

The cause of the geologically misleading gold solubilities shown in Figure 3 are apparent from the calculations that led to Figure 10. At 200°C for example, the solubility of gold as indicated in Figure 10 is 5 orders of magnitude lower than suggested by Figure 3 mainly because f_{O_2} is 10 orders of magnitude lower (which by equation (2) decreases the gold solubility by 2.25 orders of magnitude), and because the activity of H_2S is 1.5 orders of magnitude lower (which decreases the solubility of gold by 3 orders of magnitude).

Figure 11 shows the solubility of gold at 300°C as a function of salinity. Gold solubility is greatly enhanced in low salinity solutions. The reason is that much greater concentrations of the HS^- gold ligand are present in low salinity solutions.

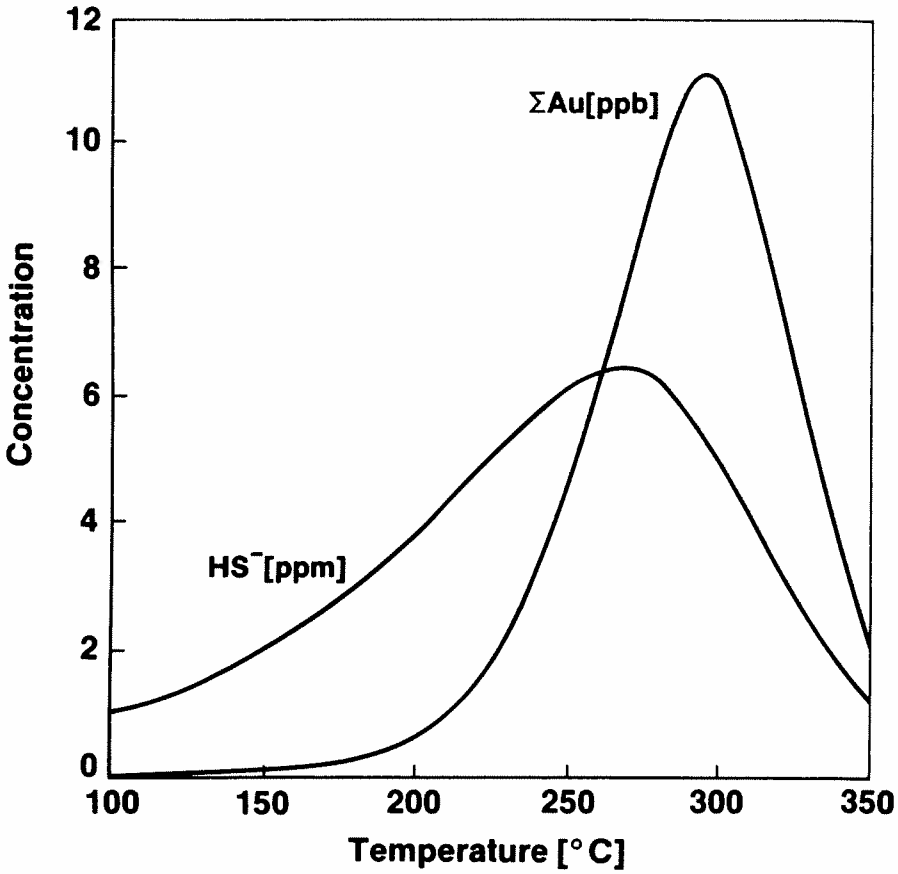

Fig. 10 *The geologic solubility of gold and HS⁻ as a function of temperature for 1000 ppm total Cl solutions. Concentrations are calculated by EQ3 for the model listed in Table 1.*

The greater abundance of HS^- in low salinity solutions can be easily understood. Ellis (1971) showed that the common silicate minerals (with which we require our solutions to be in equilibrium) control the ratio of cations like Na^+, K^+, and Ca^{++} to H^+ (Figure 12; see also Figure 4). Increasing solution salinity, by charge balance, increases the abundance of Na^+, K^+, and Ca^{++}, and hence requires the activity of H^+ to increase (i.e. the pH to decrease as shown in Figure 5). An increase in H^+ activity drives the reaction $HS^- + H^+ = H_2S$ to the right, and decreases the activity of HS^-.

The decrease in gold solubility with increasing salinity is solidly indicated by geochemical data and observations: The general decrease in pH with increasing salinity for constant temperature solutions is firmly indicated both observationally and theoretically (Figure 5). The pH dependence of the dissociation reaction for H_2S cannot be questioned.

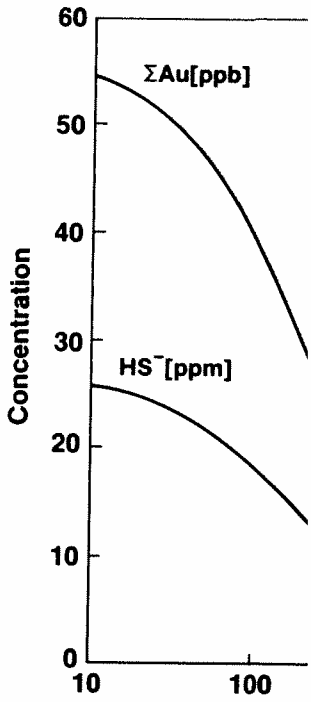

Fig. 11 *The geologic solubilit*
Concentrations calculated by
of silver as chloride complexes
of metals for which chloride l
in geothermal wells in New Z
must contribute to the solubi
should not therefore be taken
are carried as Cl complexes.

DISCUSSION

As discussed in the previous
of gold shown in Figures 10 an
changes in the Table 1 mode
solubility of gold is the possib
in the EQ3 data base could be
could become important at hi
decreasing gold solubility wi
bisulfide complexes.

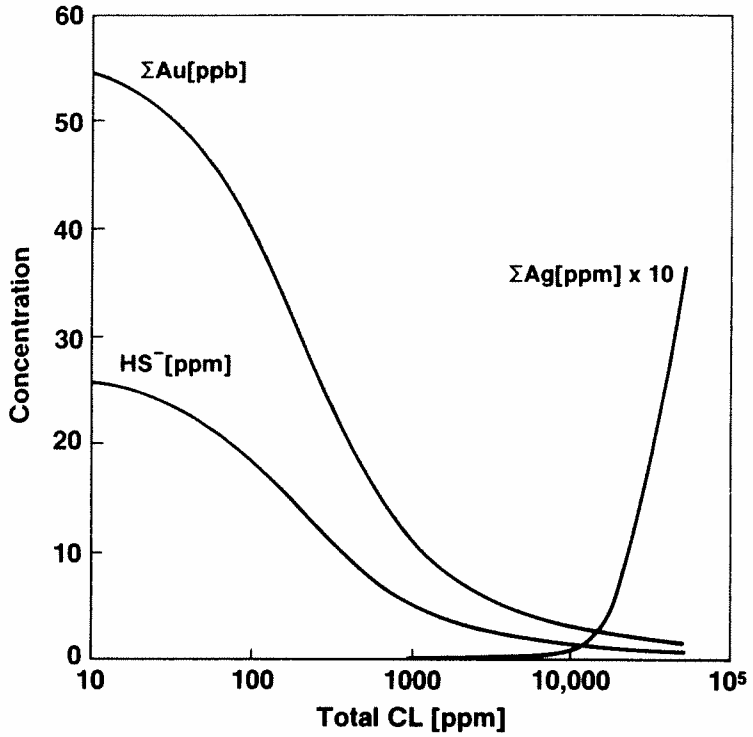

Fig. 11 *The geologic solubility of gold in 300°C solutions as a function of salinity. Concentrations calculated by EQ3 for the model listed in Table 1. The solubility of silver as chloride complexes is shown to illustrate the general salinity dependence of metals for which chloride ligands are dominant. Recent studies of precipitates in geothermal wells in New Zealand indicates that complexes other than chloride must contribute to the solubility of silver (Brown, submitted). The silver curve should not therefore be taken literally but simply as a proxy for base metals that are carried as Cl complexes.*

DISCUSSION

As discussed in the previous section, the major aspects of the geologic solubility of gold shown in Figures 10 and 11 appear to be relatively insensitive to reasonable changes in the Table 1 model. Probably the main uncertainty in the geologic solubility of gold is the possibility that gold complexes other than those included in the EQ3 data base could be important. In particular, gold chloride complexes could become important at higher salinities and reverse completely the trend of decreasing gold solubility with increasing salinity that is dictated by the gold-bisulfide complexes.

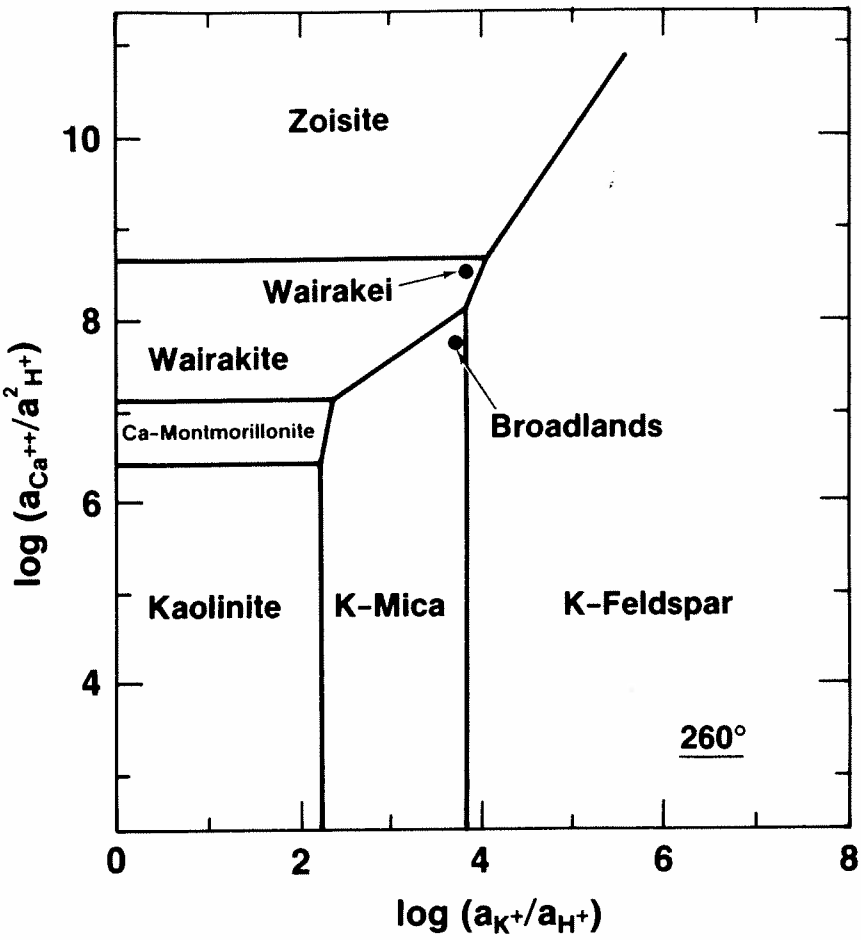

Fig. 12 *Common silicate minerals fix the ratio of cations to hydrogen. For this reason increases in salinity lead to a drop in solution pH (Ellis, 1970). Figure is simplified slightly from Ellis (1970).*

It is unlikely gold chloride complexes are important under the conditions considered in this paper. The calculations made include dissociation constants for $AuCl_2^-$ and $AuCl_4^-$ (Helgeson, 1969; see appendix). At 50,000 ppm ΣCl^-, the concentration of gold as $AuCl_2^-$ under the conditions of the Table 1 model and 300°C is only 2 parts per trillion. Henley (personal communication, 1985) has recently carried out new experiments on gold-chloride complexing and reexamined the gold-chloride solubility question. He concludes chloride complexes do not contribute to gold solubility in geothermal systems such as those considered here, although they may become important at temperatures above 500°C. Finally, gold

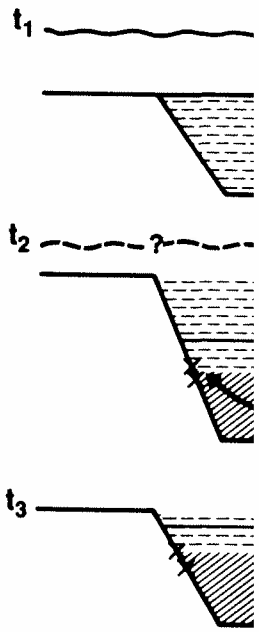

Fig. 13 *Cartoon illustrating*
in an evolving greenstone be
sion, the belt is intruded by n
deposits on the sea floor (
Infilling of the basin wit
minerals dewater, and lode g
decompress from lithostatic
text this will most likely occ
grade metamorphic bounda
Finally uplift and erosion
figuration similar to that ob
seawater which precipitate
metamorphic dewatering flui
for the different metal conte

complexes other than bisulfi
gold in natural geothermal
The dependence of gold so
tive because it can explain th
gold-poor, and base metal-po
rich and able to carry more
able to carry very little of th
chloride ligands. Conversely
base metals but less able to
vein deposits and the base-m

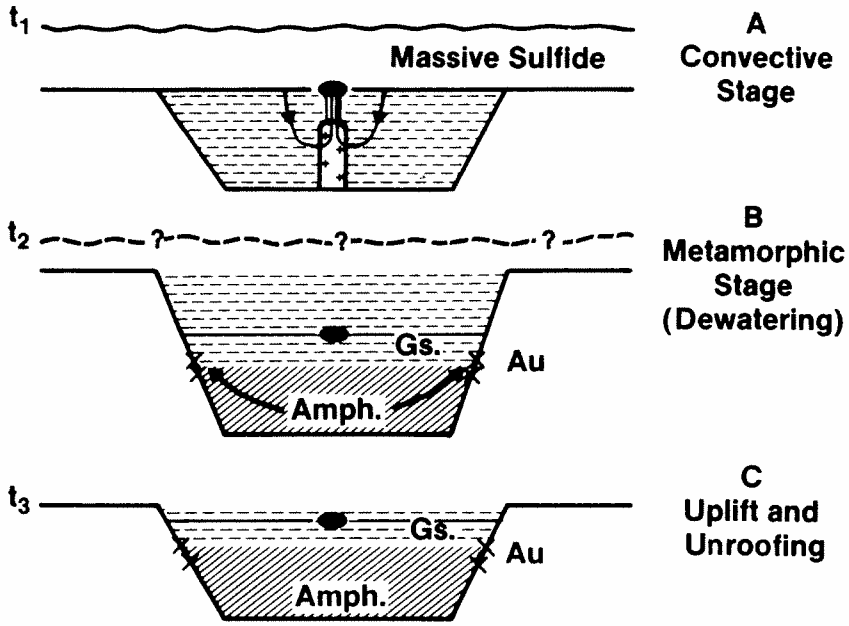

Fig. 13 *Cartoon illustrating the formation of massive sulfide and lode gold deposits in an evolving greenstone belt. During the period of most active rifting and extension, the belt is intruded by magmas, and seawater convection forms massive sulfide deposits on the sea floor (A).*

Infilling of the basin with volcanics causes burial metamorphism. Hydrous minerals dewater, and lode gold deposits are formed where these low-salinity fluids decompress from lithostatic to hydrostatic pressures. For reasons discussed in the text this will most likely occur at border faults near the amphibolite-greenstone grade metamorphic boundary (B).

Finally uplift and erosion unroofs the deposits leaving them in a spatial configuration similar to that observed (Figure 2). The difference in salinity between seawater which precipitated the massive sulfide deposits, and the low-salinity metamorphic dewatering fluids that precipitated the lode gold deposits, accounts for the different metal contents of the deposits.

complexes other than bisulfide are not needed to explain the concentrations of gold in natural geothermal systems.

The dependence of gold solubility (as bisulfide complexes) on salinity is attractive because it can explain the observed bimodal populations of base metal-rich gold-poor, and base metal-poor gold-rich deposits. Low salinity solutions are HS^- rich and able to carry more gold. At the same time they are Cl^- poor and thus able to carry very little of the base metals which are complexed and carried by chloride ligands. Conversely saline hydrothermal fluids are better able to carry base metals but less able to carry gold. The bimodal population of epithermal vein deposits and the base-metal-poor nature of lode gold deposits can thus be

explained if gold deposits are formed by the aegis of low salinity hydrothermal solutions, and base metal deposits by solutions with seawater or greater salinities.

Low salinity solutions are found primarily in two environments: subaerial where there are no evaporites, and metamorphic where hydrated minerals are broken down. These are two important environments for gold deposits (which are referred to here as epithermal and greenstone-hosted respectively).

The geographic relationship of lode gold and massive sulfide deposits in greenstone belts can be understood in terms of the natural evolution of a volcanic basin (Figure 13), Rifting causes the crust to be intruded by bimodal magmas (Figure 13a). The resulting hydrothermal convection in a submarine setting (Cathles et al, 1983) deposits massive sulfide along the axis of rifting. As the volcanic pile accumulates, temperatures in the deeper parts of the pile increase, and the pile is metamorphosed. Transition from the greenstone to amphibolite facies expels the low-salinity water from hydrated minerals (Fyfe and Kerrich, 1983). This water is expelled preferentially through major faults. Gold is precipitated as a consequence of H_2S loss where the solutions decompress from lithostatic to hydrostatic pressures. Since rock permeability seems to decrease markedly at temperatures above about 350°C (Cathles, 1983), this pressure drop is likely to occur near the greenschist-amphibolite grade metamorphic boundary. Greenstone-hosted gold deposits are indeed found near this boundary along major faults or shear zones (Figure 2, 13b).

Uplift and erosion (perhaps associated with the termination of crustal extension, Cathles et al, 1983) unroofs the greenstone belt as illustrated in Figure 12C, exposing rocks of greenstone grade, and juxtaposing massive sulfide and lode gold deposits in a geographic configuration similar to that of Figure 2.

The 300°C optimum in geologic gold solubility may explain why epithermal gold veins appear to have deposited from solutions with lower maximum temperatures than massive sulfide deposits.

SUMMARY AND CONCLUSIONS

(1) A silicate- and sulfide-buffered EQ3 model was developed that simulates the major element chemistry and pH of geothermal systems in common rock environments reasonably accurately(Table 1, Figures 4-8).

(2) Bisulfide gold complexes were incorporated in the EQ3 data base and it was verified that experimental gold solubilities are duplicated by EQ3 calculations (Figure 9).

(3) The silicate- and sulfide-buffered model was used together with the gold solubility data to investigate the solubility of gold in natural geologic environments. It was shown that the geologic solubility of gold is a maximum in low salinity solutions (Figure 11), and that the geologic solubility of gold is probably retrograde above ~300°C (Figure 10).

(4) The enhanced solubility of gold in low salinity solutions can explain the bimodal gold and base metal distributions in deposits (Figure 1).

(5) The low salinity solutions needed to form gold deposits are found primarily in subaerial environments where there are no evaporites, and in metamorphic environments where hydrated minerals are broken down. It may be useful to distinguish

gold deposited in these two s
tively. Ocean massive sulfic
is greatly reduced in fluids
(6) The distribution of l
belts can be explained if the
seawater convection, and th
metamorphic dewatering of
(7) Analysis of metal solu
as the Table 1 EQ3 model m
cations of geochemical data
quire significant modificatio
be useful for cleanly deduc

ACKNOWLEDGEMENTS

I would like to particularl
and intricacies of EQ3 and
in the appendix, Terri Bow
discussions and council on a
Wolery for producing and p
questions regarding the use
ble impact of gold chloride
bach's work on the H_2/H_2S
an iron aluminum silicate
Scott and Dick, and also to
significantly improved this
Research Company for sup

BIBLIOGRAPHY

ARNORSSON, S., 1983: Chemi
Chemical Geothermometry

ARNORSSON, S., SIGURDSSO
Waters in Iceland. I. Calculati
Acta, v.46, p1513-1532.

_____, 1983a: The Chem
Independent Variables Cont
p547-566.

_____, 1983b: The Chemi
in Geothermal Investigation

AVRAMTCHEV, L. and LEBI
Rouyn-Noranda 32D; *Gove
vices du Potential Mineral,*

BROWN, K.L., submitted: Gol
Econ. Geol.

BROWN, P.R.L., 1978: Hydrother
Sci., v. 6, p229-250.

gold deposited in these two settings as "epithermal" and "greenstone-hosted" respectively. Ocean massive sulfide deposits contain little gold because gold solubility is greatly reduced in fluids of sea water salinity.

(6) The distribution of lode gold and massive sulfide deposits in greenstone belts can be explained if the massive sulfide deposits formed by intrusive-driven seawater convection, and the lode gold deposits formed by the later low-salinity metamorphic dewatering of the accumulating volcanic pile (Figure 12).

(7) Analysis of metal solubility in silicate- and sulfide-buffered solutions such as the Table 1 EQ3 model may be generally useful in clarifying the geologic implications of geochemical data. Even if the gold complexes used here ultimately require significant modifications or additions, the geologic model of Table 1 should be useful for cleanly deducing the geologic implications of the new complexes.

ACKNOWLEDGEMENTS

I would like to particularly thank Terri Bowers for introducing me to the value and intricacies of EQ3 and for helping to refine the geochemical data base given in the appendix, Terri Bowers, Bill Hallager, and Bob Bodnar for innumerable discussions and council on a great many questions of solution chemistry, and Tom Wolery for producing and publishing the EQ3 program and for answering several questions regarding the use of it. A reviewer, Scott Wood, emphasized the possible impact of gold chloride complexes. Dick Henley drew my attention to Giggenbach's work on the H_2/H_2S ratio in geothermal fluids and the fact this suggests an iron aluminum silicate such as chlorite is a mineral buffer. I am grateful to Scott and Dick, and also to a second reviewer, Kieko Hattori, for suggestions that significantly improved this manuscript. I am indebted to the Chevron Oil Field Research Company for support of this work and for permission to publish.

BIBLIOGRAPHY

ARNORSSON, S., 1983: Chemical Equilibria in Icelandic Geothermal Systems-Implications for Chemical Geothermometry Investigations; *Geothermics, v.12, no2/3, p119-128.*

ARNORSSON, S., SIGURDSSON, S., and SVAVARSSON, H., 1982: The Chemistry of Geothermal Waters in Iceland. I. Calculations of Aqueous Speciation from 0° to 370°C; *Geochim. Cosmochim. Acta, v.46, p1513-1532.*

_____, 1983a: The Chemistry of Geothermal Waters in Iceland. II. Mineral Equilibria and Independent Variables Controlling Water Compositions; *Geochim. Cosmochim Acta, v. 47, p547-566.*

_____, 1983b: The Chemistry of Geothermal Waters in Iceland. III. Chemical Geothermometry in Geothermal Investigations; *Geochim. Cosmochim. Acta, v. 47, p567-577.*

AVRAMTCHEV, L. and LEBEL-DROLET, S., 1981: Gites Mineraux Du Quebec, Feuille Rouyn-Noranda 32D; *Government Du Quebec, Ministere de l'Energie et des Resources, Services du Potential Mineral, DPV-744.*

BROWN, K.L., submitted: Gold Deposition from Geothermal Discharges in New Zealand; *Econ. Geol.*

BROWN, P.R.L., 1978: Hydrothermal Alteration in Active Geothermal Fields; *Ann. Rev. Earth Planet. Sci., v. 6, p229-250.*

CATHLES, L.M., 1983: An Analysis of the Hydrothermal Systems Responsible for Massive Sulfide Deposition in the Hokuroku Basin of Japan; *Econ. Geol., Monograph 5, p439-487.*

CATHLES, L.M., GUBER, A.L., LENAGH, T.C., and DUDAS, F.O., 1983: Kuroko-type Massive Sulfide Deposits of Japan: Products of an Aborted Islane Arc Rift; *Econ. Geol., Monograph 5, p96-114.*

DRUMMOND, S.E.,: Boiling and Mixing of Hydrothermal Fluids: Chemical Effects on Mineral Precipitates; *PhD Thesis, The Pennsylvania State University, University Park, PA, 380p.*

DRUMMOND, S.E., and OHMOTO, H., 1985: Chemical Evolution and Mineral Deposition in Boiling Hydrothermal Systems; *Econ. Geol., v. 80, p126-147.*

ELDER, J., 1981: Geothermal Systems, Academic Press; *New York, 508 p.*

ELLIS, A.J., 1970: Quantitative Interpretation of Chemical Characteristics of Hydrothermal Systems; *Geothermics, Special issue 2, v 2, part 1, p516-528.*

ELLIS, A.J. and GIGGENBACH, W.F., 1971: Hydrogen Sulfide Ionization and Sulphur Hydrolysis in High Temperature Solutions; *Geochim. Cosmochim. Acta, v. 35, p247-260.*

FYFE, W.S. and KERRICH, R., 1983: Gold: Natural Concentration Processes; in *"Gold ;82: The Geology, Geochemistry and Genesis of Gold Deposits", proceedings of the symposium Gold '82, University of Zimbabwe, Geological Society of Zimbabwe, p99-127.*

GIGGENBACH, W.F., 1980: Geothermal Gas Equilibria; *Geochim. Comochim. Acta, v. 44, p2021-2032.*

GIGGENBACH, W.F., 1981: Geothermal Mineral Equilibria; *Geochim. Cosmochim. Acta, v. 45, p393-410.*

HELGESON, H.C., KIRKHAM, D.H. and FLOWERS, G.C., 1981: Theoretical Predictions and Pressures; *Amer. Jour. Sci., 267, p729-804.*

HELGESON, H.C., DELANEY, J.M., NESBITT, H.W., and BIRD, D.K., 1978: Summary and Critique of the Thermodynamic Properties of the Rock-Forming Minerals; *Amer. Jour. Sci., v. 278A, p1-228.*

HELGESON, H.C., KIRKHAM, D.H. and FLOWERS, G.C., 1981: Theoretical Predictions of the Thermodynamic Behavior of Aqueous Electrolytes at High Pressures and Temperatures: IV. Calculation of Activity Coefficients, Osmotic Coefficients, and Apparent Molal and Standard Relative Partial Molal Properties to 600°C and 5kb; *Amer. Jour. Sci., v. 281, p1249-1516.*

HENLEY, R.W., TRUESDELL, A.H., and BARTON, P.B., 1984: Fluid-Mineral Equilibria in Hydrothermal Systems; *Reviews in Economic Geology, V. 1; Soc. Econ. Geol., 267p.*

HENLEY, R.W., and HEDENQUIST, J.W., 1983: An Introduction to the Geochemistry of Active and Fossil Geothermal Systems; in *Proceedings of a Field Conference on Epithermal Environments in New Zealand, R.W. Henley and P. Roberts Convenors, Feb. 23-30.*

PLUMMER, L.M., and BUSENBERG, E., 1982: The Solubilities of Calcite, Aragonite, and Vaterite in CO_2-H_2O Solutions Between 0 and 90°C, and an Evaluation of the Aqueous Model of the System $CaCO_3$-CO_2-H_2O; *Geochim. Cosmochim. Acta, v. 46, p1011-1040.*

RAGNARSDOTTIR, K.V., WALTHER, J.V., and ARNORSSON, S., 1984: Description and Interpretation of the Composition of Fluid and Alteration in the Geothermal System, at Svartsengi, Iceland; *Geochim. Cosmochim. Acta, v. 48, p1535-1553.*

REED, M. and SPYCHER, N., 1984: Calculation of pH and Mineral Equilibria in Hydrothermal Waters with Application to Geothermometry and Studies of Boiling and Dilution; *Geochim. Cosmochim. Acta, v. 48, p1479-1492.*

SEWARD, T.M., 1973: Thio Complexes of Gold and the Transport of Gold in Hydrothermal Solutions; *Geochim. Cosmochim. Acta, v. 37, p379-399.*

SEWARD, T.M., 1976: The Stability of Chloride Complexes of Silver in Hydrothermal Solutions up to 350°C; *Geochim. Cosmochim. Acta, v. 40, p1329-1341.*

TREMAINE, P.R., and LeBLANC, J.C., 1980: The Solubility of Iron (+2) ion in water and the hydrolysis and oxidation of iron (2+) ion in water to 300°C; *J. Solution Chem., v. 9, p415-442.*

WOLERY, T.J., 1983: EQ3NR, a computer program for geochemical speciation-solubility calculations: User's guide and documentation; *Lawrence Livermore Laboratory, UCRL-53414, 191p.*

APPENDIX: The The

Most of the thermody
in our calculations is fror
et al (1978, 1981). The da
stants is from Seward (1
were deduced from Sew
the complex as AuHS° (
for H_2CO_3 has been ex
Busenberg, 1982). We ex
et al's (1984, Table 7.3) an
fit Giggenbach's (1981) th
tion constant for H_2S at
et al 1984, Table 8.1) fror
to 276°C (Ellis and Gigg
order of magnitude larger
dissociation constants are
tion reactions were adju
Terry Bowers, acting as a
tion constants listed belo
reported by Tremaine an

Several comments shou
ed in Table A-1. First the
concentrations predicted
a product of the pyrite diss
tion constant was an ord
350°C (as it was in the un
would predict an H_2S co
Figure 6. The HS^- and gc
tions in the H_2S dissocia
the observed and predict
in the 350°C H_2S dissoci
extrapolation of experim
remodified in this fashion
be unchanged.

Second the iron hydrox
the geologic solubility of
stants in the unmodified E
in Wolery's EQ3 data ba
Tremain and LeBlanc's da
ppm concentrations of irc
This hydroxide iron solu
precipitation of a magnitu
The iron hydroxide dissoc
concentrations under the
iron solubility makes it d
appealing to processes oc
the vein walls).

APPENDIX: The Thermodynamic data base

Most of the thermodynamic data for water, aqueous species, and minerals used in our calculations is from Wolery (1983) and is based on Helgeson (1969), Helgeson et al (1978, 1981). The data for silver chloride and gold bisulfide dissociation constants is from Seward (1976 and 1973). The dissociation constants for $HAu(HS)_2^\circ$ were deduced from Seward (1973, Figure 6; note Seward's Figure 7 misidentifies the complex as $AuHS^\circ$ (Seward, pers. comm., 1985). The dissociation constant for H_2CO_3 has been experimentally determined only to 218°C (Plummer and Busenberg, 1982). We extrapolate the data to higher temperatures between Henley et al's (1984, Table 7.3) and Helgeson's (1969) extrapolations so as to approximately fit Giggenbach's (1981) theory and geothermal data (see Figure 8). The dissociation constant for H_2S at 350°C is obtained using a smooth extrapolation (Henley et al 1984, Table 8.1) from experimental data covering the temperature range 20° to 276°C (Ellis and Giggenbach, 1971, Table 1). This dissociation constant is an order of magnitude larger than that in Wolery's (1983) EQ3 data base. Iron hydroxide dissociation constants are taken from Tremaine and LeBlanc (1980). Their dissociation reactions were adjusted to allow encorporation into the EQ3 data base by Terry Bowers, acting as a consultant to Chevron. Terry demonstrated the dissociation constants listed below accurately simulate the experimental iron solubilities reported by Tremaine and LeBlanc.

Several comments should be made regarding the modified data base summarized in Table A-1. First the change in the H_2S dissociation constant affects the H_2S concentrations predicted by the pyrite-daphnite-magnetite buffer because HS^- is a product of the pyrite dissolution reaction in the EQ3 data base. If the H_2S dissociation constant was an order of magnitude smaller than indicated in Table A-1 at 350°C (as it was in the unmodified data base), the pyrite-daphnite-magnetite buffer would predict an H_2S concentration at 350°C close to the Giggenbach trend in Figure 6. The HS^- and gold concentrations at 350°C are unchanged by modifications in the H_2S dissociation constant, however. The better agreement between the observed and predicted H_2S concentrations in Figure 6 suggests a decrease in the 350°C H_2S dissociation constant may be reasonable, even though smooth extrapolation of experimental data suggests otherwise. If the data base were remodified in this fashion, the retrograde solubility of gold above 300°°C would be unchanged.

Second the iron hydroxide complexes listed in Table A-1 significantly decrease the geologic solubility of iron indicated by the iron hydroxide dissociation constants in the unmodified EQ3 data base. The iron hydroxide dissociation constants in Wolery's EQ3 data base do not produce iron concentrations that agree with Tremain and LeBlanc's data. Wolery's iron hydroxide dissociation constants predict ppm concentrations of iron under the geologic conditions of the Table 1 model. This hydroxide iron solubility is maximum at 300°C and would allow pyrite precipitation of a magnitude that could account for the pyrite in gold vein deposits. The iron hydroxide dissociation constants listed in Table A-1 predict very low iron concentrations under the geologic conditions of the Table 1 model. This very low iron solubility makes it difficult to account for the pyrite in gold veins without appealing to processes occuring in the vein itself (such as leaching of iron from the vein walls).

Table A-1

Log dissociation constants for aqueous species added or modified in the EQ3 data base for this study.

	100°	150°	200°	250°	300°	350°C
$H_2CO_3 = 2H^+ + CO_3^=$	-16.61	-17.04	-17.84	-19.26	-21.55	-24.96
$H_2S = H^+ + HS^-$	-6.62	-6.78	-7.15	-7.61	-8.05	-8.37
$Au(HS)_2^- = Au^+ + 2HS^-$	-26.47	-23.40	-21.07	-19.41	-18.31	-17.70
$Au_2(HS)_2S^= = 2Au^+ + 2\ HS^- + S^=$	-47.43	-40.85	-35.35	-31.05	-28.05	-26.48
$HAu(HS)_2^0 = Au^+ + H^+ + 2HS^-$	-30.16	-27.81	-25.86	-24.36	-23.36	-22.91
$AuCl_2^- = Au^+ + 2Cl^-$	-7.49	-6.49	-6.25	-6.29	-6.17	-5.42*
$AgCl = Ag^+ + Cl^-$	-2.94	-2.82	-2.87	-3.11	-3.55	-4.21
$AgCl_2^- = Ag^+ + 2Cl^-$	-4.54	-4.40	-4.51	-4.86	-5.51	-6.51
$AgCl_3^= = Ag^+ + 3Cl^-$	-3.85	-3.73	-3.67	-3.67	-3.67	-3.67
$AgCl_4^{3-} = Ag^+ + 4Cl^-$	-1.94	-1.79	-1.61	-1.40	-1.19	-1.00
$Fe(OH)^+ + H^+ = Fe^{++} + H_2O$	8.78	8.09	7.56	7.12	6.96	6.50
$Fe(OH)_2 + 2H^+ = Fe^{++} + 2H_2O$	17.15	15.44	14.09	12.99	12.09	11.21
$Fe(OH)_3^- + 3H^+ = Fe^{++} + 3H_2O$	28.11	25.63	23.68	22.10	20.80	19.50
$Fe(OH)_3 + 2H^+ = Fe^{++} + 2.5\ H_2O + 0.25\ O_2(g,aq)$	3.94	3.80	3.69	3.54	3.24	2.75
$Fe(OH)_4^- + 3H^+ = Fe^{++} + 3.5\ H_2O + 0.25\ O_2(g,aq)$	12.89	12.54	12.09	11.74	11.28	10.65

* Unchanged from Helgeson(1969) except for slight shifts caused by the polynomial fit of EQTL (see Wolery, 1983).